

# Single-photon quantum nondemolition detectors constructed with linear optics and projective measurements

Pieter Kok\*, Hwang Lee, and Jonathan P. Dowling  
Quantum Computing Technologies Group, Section 367  
Jet Propulsion Laboratory, California Institute of Technology  
Mail Stop 126-347, 4800 Oak Grove Drive, Pasadena, California 91109

Optical quantum nondemolition devices can provide essential tools for quantum information processing. Here, we describe several optical interferometers that signal the presence of a single photon in a particular input state without destroying it. We discuss both entanglement-assisted and non-entanglement-assisted interferometers, with ideal and realistic detectors. We found that existing detectors with 88% quantum efficiency and single-photon resolution can yield output fidelities of up to 89%, depending on the input state. Furthermore, we construct expanded protocols to perform QND detections of single photons that leave the polarization invariant. For detectors with 88% efficiency we found polarization-preserving output fidelities of up to 98.5%.

PACS numbers: 42.25.Hz, 42.79.Ta, 42.50.Dv, 03.65.Ud, 03.67.-a

Quantum Nondemolition (QND) devices measure observables and couple the back-action noise only to the conjugate of the measured quantity. The measurement projects the system under scrutiny onto an eigenstate of the measured observable, and repeated QND measurements yield the same outcome as the initial one. These devices therefore closely resemble ideal von Neumann measurements [1]. QND devices can be exploited, for example, to improve the sensitivity in gravitational wave detection, to create entanglement on demand, and to implement QND-based quantum computing using projective measurements (see Ref. [2–6]).

In quantum optics, we usually consider QND devices in the context of photon-number measurements. There, we have the added complication of ultimate demolition; common photodetectors destroy the photons they detect. To avoid this demolition, there exist QND proposals using special components such as Kerr media, parametric amplifiers, cold atoms in magneto-optical traps, or cavity quantum electrodynamics [7]. However, these protocols generally require strong nonlinearities or are highly frequency-dependent.

In a recent experiment, Nogues *et al.* performed a single-photon QND measurement of a weak cavity field. They used the resonant coupling between the field and atoms moving through the cavity [8]. When there was a single photon in the cavity, the initial atom-field state  $|g, 1\rangle$  evolved in time according to  $|g, 1\rangle \rightarrow \cos(\Omega t/2)|g, 1\rangle + \sin(\Omega t/2)|e, 0\rangle$ . Here,  $|g\rangle$  and  $|e\rangle$  are the ground state and the excited state of the atoms. The photon-number field states are  $|0\rangle$  and  $|1\rangle$ , and  $\Omega$  is the Rabi frequency. When  $t = 2\pi/\Omega$ , the initial state  $|g, 1\rangle$  acquired a phase shift of  $\pi$ . By contrast, when there were no photons in the cavity, the state  $|g, 0\rangle$  would not accumulate a phase shift. The relative phase-shift was then measured with a Ramsey interferometer by coupling  $|g\rangle$  with another atomic level  $|g'\rangle$  [8].

Since a Ramsey interferometer involves atomic transi-

tions, this QND device depends strongly on the frequency of the field. The next step is therefore to investigate simple *frequency independent* QND devices. One possibility is the use of non-deterministic interferometric QND detection.

This paper is organized as follows: in section I we describe the conventional interferometric QND device that uses Kerr nonlinearities, and we also present a simple teleportation-based scheme to detect the presence of a single photon. In section II we introduce an interferometric scheme based on linear optics and projective measurements, and we study the effect of inefficient detectors and degraded single-photon auxiliary input states. The difference between this and the teleportation-based protocol is that this scheme can detect a single photon out of 0, 1 or 2 photons, whereas the teleportation-based scheme can tell the difference between only 0 and 1 photon. This difference is critical for linear optical quantum computing. Finally, in section III we construct a modified protocol to perform QND detections of single photons that leave the polarization invariant.

## I. INTERFEROMETRIC QND

In this section we present the conventional interferometric quantum nondemolition scheme that uses the Kerr effect [9]. This scheme is based on a phase measurement, and the fundamental phase error puts a bound on the strength of the Kerr nonlinearity. Secondly, we present a simple scheme to achieve single-photon QND detection with linear optics based on teleportation.

### A. Kerr nonlinearities

It is widely believed that to create an interferometric, photon-number quantum nondemolition device, you need

a Kerr medium [9]. A QND device based on such a nonlinearity works as follows (see Fig. 1): let  $\hat{a}^\dagger$ ,  $\hat{b}^\dagger$  and  $\hat{a}$ ,  $\hat{b}$  be the creation and annihilation operators for two optical modes  $a$  and  $b$ , satisfying the commutation relations

$$[\hat{a}, \hat{a}^\dagger] = [\hat{b}, \hat{b}^\dagger] = 1 \quad \text{and} \quad [\hat{a}, \hat{b}] = [\hat{b}, \hat{a}] = 0. \quad (1)$$

The following Hamiltonian describes the effect of a Kerr cell on modes  $a$  and  $b$ :

$$\hat{H}_{\text{Kerr}} = \kappa \hat{a}^\dagger \hat{a} \hat{b}^\dagger \hat{b}. \quad (2)$$

This interaction induces a phase-shift in mode  $a$  (or  $b$ ), depending on the number of photons in mode  $b$  (or  $a$ ). In general the mode transformations are

$$\hat{a}^\dagger \rightarrow \hat{a}^\dagger e^{-i\tau \hat{n}_b} \quad \text{and} \quad \hat{b}^\dagger \rightarrow \hat{b}^\dagger e^{-i\tau \hat{n}_a}, \quad (3)$$

where the dimensionless characteristic interaction strength  $\tau \equiv \kappa t / \hbar$  is based on the interaction time  $t$  and the number operator  $\hat{n}_a$  (defined by  $\hat{n}_a \equiv \hat{a}^\dagger \hat{a}$  and similarly for  $\hat{n}_b$ ). By monitoring the phase shift in mode  $a$  using a Mach-Zehnder interferometer (i.e., homodyne detection), we can determine the photon-number in mode  $b$  *without* destroying the photons. The phase of the output state is completely uncertain, which can be understood from the number–phase uncertainty relation. For a detailed description of general nonlinear interferometers, see e.g., the article by Sanders and Rice [11].

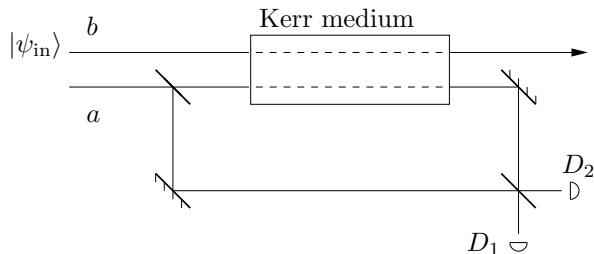


FIG. 1. A photon-number quantum nondemolition device based on the Kerr effect. A photon in mode  $b$  changes the phase of the photon in mode  $a$ . The Mach-Zehnder interferometer is tuned in such a way that a detector click in  $D_1$  signals no photon, and a click in  $D_2$  signals one photon.

We can measure any photon number in mode  $b$  by estimating the induced phase in mode  $a$ . However, the phase estimation process has a fundamental error  $\Delta\phi$  (where  $\phi = \tau \hat{n}_b$  is the induced phase). To attain single-photon resolution, this error should be strictly smaller than the phase shift induced by a single photon, or  $\Delta\phi < \tau$ . Of course, we are not restricted to single-photon interferometry to estimate this phase shift. We can use Heisenberg-limited interferometry to obtain a lower bound on the strength of the Kerr nonlinearity [12].

For example, we may use so-called “noon states” [13]  $(|N, 0\rangle + |0, N\rangle) / \sqrt{2}$ , where  $|0\rangle$  and  $|N\rangle$  are the vacuum and the  $N$ -photon Fock states respectively. If the state

inside the Mach-Zehnder interferometer has this form, we obtain the following bound for the phase uncertainty and the strength of the Kerr effect:

$$\tau > \Delta\phi = \frac{\pi}{2} \frac{1}{N}. \quad (4)$$

When we use single-photon interferometry ( $N=1$ ), we retrieve the well-known value of  $\tau = \pi/2$ . In experiments with coherent states, the phase is determined by the standard limit, which yields  $\tau > \pi / (2\sqrt{\langle n \rangle})$ . Here,  $\langle n \rangle$  is the average photon number. By using high-intensity laser beams, Grangier *et al.* demonstrated Kerr-based QND measurements with small nonlinearities [2].

Due to the typically small values of the nonlinearity, the Kerr-based single-photon QND device is not practical. The  $\chi^{(3)}$  coupling involved is extremely weak ( $\kappa \propto 10^{-16} \text{ cm}^2 \text{ sV}^{-2}$  [14]), and such a detection device would necessarily have an exceedingly small efficiency. Recently, large Kerr nonlinearities were constructed using slow light, but these techniques are still highly experimental [15]. We therefore wish to bypass the use of weak  $\chi^{(3)}$  nonlinearities and construct a single-photon QND device with more user-friendly optical elements. In this paper, we show that under certain relaxing conditions only linear optics and projective measurements suffice.

## B. Strength of the nonlinearity

Before we continue, we derive the strength of the Kerr nonlinearity in terms of the dimensionless coupling constant  $\tau$  of Eq. (4). A wave travelling through a medium accumulates a phase shift  $\varphi$  that in the scalar approximation is given by  $\varphi = \vec{k} \cdot \vec{x} = kLn$ . The wave number is denoted by  $k$ ,  $L$  is the length of the medium, and  $n$  is the index of refraction. In general,  $n$  can be written in terms of the higher-order nonlinearities as

$$n^2 = 1 + \chi^{(1)} + \chi^{(2)}E + \chi^{(3)}E^2 + \dots, \quad (5)$$

where  $E$  is the electric field strength of the wave. Here, we are interested in the third-order ( $\chi^{(3)}$ ) contribution to the phase shift, and we choose  $\chi^{(1)} = \chi^{(2)} = 0$ . The total phase shift then becomes

$$\varphi = kL\sqrt{1 + \chi^{(3)}E^2} \approx kL \left( 1 + \frac{\chi^{(3)}E^2}{2} \right). \quad (6)$$

The phase shift  $\tau$  due to the Kerr effect is then

$$\tau = \frac{1}{2}kL\chi^{(3)}E^2. \quad (7)$$

Since  $\chi^{(3)}$  is a constant of the material, we need only to determine  $E$  for a single photon to find the numerical

value of  $\tau$ . In the appropriate units the electric field of a single photon with central frequency  $\omega$  becomes [10]

$$E = \sqrt{\frac{\hbar\omega}{2\epsilon_0 V}}, \quad (8)$$

where  $\epsilon_0$  is the permittivity of the vacuum and  $V$  the volume of the medium that induces the phase shift. This yields

$$\tau = \frac{\hbar\omega^2 \Delta t \chi^{(3)}}{4\epsilon_0 V}. \quad (9)$$

Here, we used  $k = \omega/c$  and  $\Delta t = L/c$ , where  $c$  is the speed of light in vacuum. When we choose the typical values of  $\omega = 3 \cdot 10^{15}$  rad s<sup>-1</sup>,  $\Delta t = 3 \cdot 10^{-11}$  s,  $\chi^{(3)} = 2 \cdot 10^{-22}$  m<sup>2</sup> V<sup>-2</sup>, and the size of the Kerr medium is 1 cm  $\times$  0.1 cm<sup>2</sup>, the value for the dimensionless coupling becomes  $\tau \approx 10^{-18}$ .

### C. Teleportation-based protocol

One simple way to perform a single-photon measurement without destroying the photon is to use single-photon quantum teleportation [16]. In Fig. 2 we show how such a protocol would work. The input state  $|\psi_{\text{in}}\rangle$  may be in an arbitrary superposition of zero and one photon with a particular polarization. A maximally polarization-entangled photon-pair (e.g., created by a parametric down-converter, or PDC) serves as the quantum channel, and a detector coincidence in  $D_1$  and  $D_2$  identifies a (partial) Bell measurement. This detector coincidence also signals the presence of a single photon in the input and the output state. It is easily seen that a vacuum input state ( $|\psi_{\text{in}}\rangle = |0\rangle$ ) can never lead to a two-fold detector coincidence, and that a low efficiency pair production in the down-converter does not affect the fidelity of the single-photon QND device.

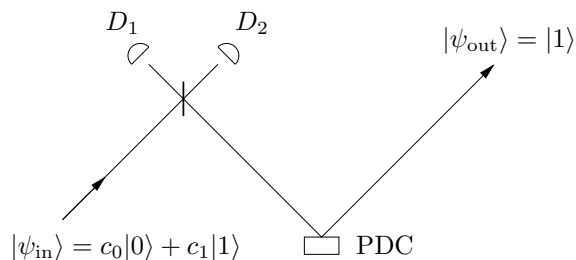


FIG. 2. Teleportation-based single-photon quantum non-demolition device. A detector coincidence in  $D_1$  and  $D_2$  signals the presence of a photon in  $|\psi_{\text{in}}\rangle$  and  $|\psi_{\text{out}}\rangle$ . This scheme breaks down when there is potentially more than one photon in the input state.

However, this scheme breaks down in the more interesting case where the input state is of the form

$$|\psi_{\text{in}}\rangle = c_0|0\rangle + c_1|1\rangle + c_2|2\rangle. \quad (10)$$

The two-photon term will end up contributing to the coincidences in  $D_1$  and  $D_2$  when the output of the down-converter is vacuum. This scheme therefore falsely identifies the presence of a single photon conditioned on a detector coincidence.

In the next section we shall develop an interferometer that faithfully signals the presence of a single photon in such an input state. In section III A we shall give a more detailed analysis of the teleportation-based QND device, including unknown polarizations of the input state. In the next section we study an interferometric scheme that does work on an input state given by Eq. (10).

## II. LINEAR OPTICS AND PROJECTIVE MEASUREMENTS

Our main goal in this section is to describe an interferometric single-photon QND device that non-destructively signals the presence of a single photon when the input state is of the form of Eq. (10). Note that this is not a full QND measurement of the photon-number observable since it works for only the lowest three numbers (0, 1, and 2). However, it can still play an important rôle in linear optical quantum computing, where up to only two-photon states are used, such as the recently proposed linear optical quantum computation scheme by Knill, Laflamme and Milburn [6].

To construct such a dressed-down QND device, we consider the following two relaxing conditions: Firstly, when the device does *not* signal the presence of a single photon, the output state may be severely disturbed; we therefore essentially propose a device for protocols using single-photon post-selection. Secondly, we do not require a 100% efficiency for the QND device. It is sufficient to create a probabilistic device that has a lower effective efficiency. Under these conditions, we show how to build a single-photon QND device.

The interferometric QND detector has possible applications in the construction of quantum logic gates [17], single-photon triggers [18], detectors of the quantum Zeno effect [19], quantum repeaters [20] and to fundamental tests of quantum mechanics [21]. In the following sections we shall describe the interferometer by specifying the transformation properties of the creation operators of the different optical modes, and we calculate the efficiency and fidelity in the presence of detector losses. Finally, we consider imperfections in the single-photon probe sources.

## A. The interferometer

Consider the interferometric setup in Fig. 3. The beam splitters are chosen asymmetric: When a photon is transmitted it will not experience a phase shift, but when a photon is reflected it accumulates a relative minus sign, depending on the side it reflects off. The arrow in Fig. 3 indicates the preferred direction:

$$\hat{a}^\dagger \rightarrow \frac{\hat{p}^\dagger + \hat{q}^\dagger}{\sqrt{2}} \quad \text{and} \quad \hat{b}^\dagger \rightarrow \frac{\hat{q}^\dagger - \hat{p}^\dagger}{\sqrt{2}}. \quad (11)$$

You can convert these transformation rules into other representations of the beam splitter by using three phase shifts. For example, a phase shift of  $\pi/2$  in modes  $b$  and  $q$ , and a phase shift of  $\pi$  in mode  $p$  yields

$$\hat{a}^\dagger \rightarrow \frac{-\hat{p}^\dagger + i\hat{q}^\dagger}{\sqrt{2}} \quad \text{and} \quad \hat{b}^\dagger \rightarrow \frac{i\hat{p}^\dagger - \hat{q}^\dagger}{\sqrt{2}}.$$

In the rest of the paper we shall use Eq. (11). The creation operators  $\hat{a}^\dagger$ ,  $\hat{b}^\dagger$ ,  $\hat{c}^\dagger$  and  $\hat{d}^\dagger$  of the input modes  $a$ ,  $b$ ,  $c$  and  $d$  then transform into

$$\hat{a}^\dagger \rightarrow \frac{\hat{a}'^\dagger - \hat{c}'^\dagger}{\sqrt{2}}, \quad (12a)$$

$$\hat{b}^\dagger \rightarrow \frac{\hat{b}'^\dagger + \hat{c}'^\dagger}{\sqrt{2}}, \quad (12b)$$

$$\hat{c}^\dagger \rightarrow \frac{1}{2} (\hat{a}'^\dagger + \hat{b}'^\dagger + \hat{c}'^\dagger + \hat{d}'^\dagger), \quad (12c)$$

$$\hat{d}^\dagger \rightarrow \frac{1}{2} (\hat{b}'^\dagger - \hat{a}'^\dagger + \hat{d}'^\dagger - \hat{c}'^\dagger). \quad (12d)$$

We shall now study the behaviour of the QND device.

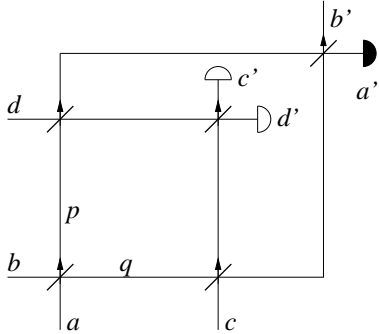


FIG. 3. Interferometric QND measurement device for single-photon detection. The device signals the presence of a single photon in mode  $a$  by giving a detector coincidence in modes  $c'$  and  $d'$  and *no* count in mode  $a'$ . The outgoing mode  $b'$  then is in a single-photon state.

Let the input state be

$$|\Psi_{\text{in}}\rangle = |\psi_{\text{in}}, 0, 1, 1\rangle_{abcd}, \quad (13)$$

where  $|\psi_{\text{in}}\rangle$  is defined by Eq. (10). In terms of creation operators, this state can be written as

$$|\Psi_{\text{in}}\rangle = \sum_{k=0}^2 c_k \hat{a}^{\dagger k} \hat{c}^\dagger \hat{d}^\dagger |0\rangle. \quad (14)$$

Using Eqs. (12c) and (12d), the two probe photons in modes  $c$  and  $d$  transform into [see Eq. (14)]

$$\hat{c}^\dagger \hat{d}^\dagger \rightarrow \frac{1}{4} (\hat{b}'^{\dagger 2} - \hat{a}'^{\dagger 2} + \hat{d}'^{\dagger 2} - \hat{c}'^{\dagger 2} - 2\hat{a}'^\dagger \hat{c}'^\dagger + 2\hat{b}'^\dagger \hat{d}'^\dagger). \quad (15)$$

Based on one photon in mode  $c$ , one in mode  $d$ , and nothing in  $a$  and  $b$ , we can never have a coincidence in modes  $c'$  and  $d'$ : there is no  $\hat{c}'^\dagger \hat{d}'^\dagger$  component in Eq. (15). Similarly, when the input mode is in a two-photon state  $|2\rangle$  ( $k=2$ ), the operator transformation from Eq. (12a) yields

$$\hat{a}'^{\dagger 2} \rightarrow \frac{1}{2} (\hat{a}'^{\dagger 2} - 2\hat{a}'^\dagger \hat{c}'^\dagger + \hat{c}'^{\dagger 2}). \quad (16)$$

The only detector coincidence in modes  $c'$  and  $d'$  due to a two-photon input is obtained when the  $2\hat{b}'^\dagger \hat{d}'^\dagger$  contribution from Eq. (15) is combined with the  $2\hat{a}'^\dagger \hat{c}'^\dagger$  contribution of Eq. (16) to yield  $\hat{a}'^\dagger \hat{b}'^\dagger \hat{c}'^\dagger \hat{d}'^\dagger$ . However, post-selecting on vacuum in mode  $a'$  rules out this two-photon contribution to the detector coincidence in  $c'$  and  $d'$ .

Finally, a single photon in mode  $a$  yields a contribution  $\hat{b}'^\dagger \hat{c}'^\dagger \hat{d}'^\dagger$  [ $k=1$  in Eq. (14)]—that is, there is a coincidence event in modes  $c'$  and  $d'$ , *and* there is a photon in the output mode  $b'$ . These properties constitute our single-photon quantum nondemolition device. The efficiency of this interferometric QND device with 50:50 beam splitters is  $1/8$ . This can be easily seen by determining the prefactor of the contribution  $\hat{b}'^\dagger \hat{c}'^\dagger \hat{d}'^\dagger$ , which yields  $1/(2\sqrt{2})$ . The square of this amplitude is  $1/8$ . We can optimize this probability by changing the transmission coefficients  $T$  of the beam splitters in modes  $c$  and  $d$ . When we choose  $T = 1/3$ , the probability of success becomes  $4/27$ .

## B. Realistic detectors

For interferometers that operate at the low photon-number level, the fidelity of the output state depends critically on the performance of the photodetectors. The same is true for our single-photon QND device. So far we have implicitly assumed that we have ideal detectors—that is, the detectors give the correct photon number in a mode every time they are used. Such detectors are said to have unit efficiency and perfect single-photon resolution [22]. However, these detectors do not exist. It is therefore important to study how imperfections in the detection process affect the fidelity of the output state.

First, we define the fidelity of the output state of the interferometer as

$$F \equiv \text{Tr}[\rho_{\text{out}}|\psi\rangle\langle\psi|] \leq 1, \quad (17)$$

where  $|\psi\rangle$  is the expected pure state (in our case the single-photon state  $|1\rangle$ ), conditioned on the detector signature) and  $\rho_{\text{out}}$  the (generally mixed) output state. When  $F = 1$ , the QND device works perfectly. We shall now study how detector inefficiencies affect the fidelity.

Suppose that the detectors have a non-unit quantum efficiency  $\eta$ , i.e., the probability that a photon is detected is  $\eta^2$ . Furthermore, suppose that the detectors have perfect single-photon resolution. It can then still mistake a two-photon state for a single photon when one of the photons is not detected. Kim *et al.* developed such detectors, which operate at about 7 K with a quantum efficiency of  $\eta^2 = 88\%$  [23]. We shall next calculate the fidelity of the single-photon QND device using these detectors.

Mathematically, we model detection as follows: The outgoing state  $\rho_{\text{out}}$  is obtained by tracing over the (pure) multi-mode output state just before detection  $|\Psi\rangle$  and the positive operator-valued measure (POVM)  $\hat{E}_{\vec{n}}$ :

$$\rho_{\text{out}} = \text{Tr} \left[ \hat{E}_{\vec{n}} |\Psi\rangle\langle\Psi| \right], \quad (18)$$

where  $\vec{n} = (n_1, \dots, n_M)$  denotes the detector signature of finding  $n_k$  photons in mode  $k$ . The total number of detected modes  $M$  must be smaller than the total number of modes  $N$  in the interferometer. Our task is to find a general expression for  $\hat{E}_{\vec{n}}$ .

Since, in our approximation, detectors operate on single modes, the POVM  $\hat{E}_{\vec{n}}$  will factor into  $\hat{E}_{n_1} \otimes \dots \otimes \hat{E}_{n_M}$ , where the separate POVM's  $\hat{E}_{n_k}$  are the measures for single-mode detectors. When the detectors are ideal, the POVM's reduce to projection operators

$$\hat{E}_{n_k}^{(\text{ideal})} = |n_k\rangle\langle n_k|. \quad (19)$$

In general, the single-mode detector POVM has the form

$$\hat{E}_n = \sum_{k=n}^{\infty} d_{n,k} |k\rangle\langle k|, \quad (20)$$

where the sum runs from  $n$ , since in our model the detector cannot detect more photons than there are present in the incoming beam. In other words, we discard dark counts. Furthermore, for  $\hat{E}_n$  to be a proper POVM, we require that

$$\sum_{n=0}^{\infty} \hat{E}_n = \mathbb{1}, \quad (21)$$

where  $\mathbb{1}$  is the identity operator.

To find the expression for  $\hat{E}_n$ , we model the detector loss by a beam splitter with transmission amplitude  $\eta$ .

In this model we assume that the detector detects photons independently. The reflected photons represent the loss, and we take the trace over the corresponding output mode. The POVM then becomes ( $\tilde{\eta} \equiv \sqrt{1 - \eta^2}$ ) [24]

$$\begin{aligned} \hat{E}_n &= \text{Tr}_b \left[ \frac{1}{n!} (\eta \hat{a}^\dagger + \tilde{\eta} \hat{b}^\dagger)^n |0\rangle\langle 0| (\eta \hat{a} + \tilde{\eta} \hat{b})^n \right] \\ &= \sum_{k=0}^n \binom{n}{k} \eta^{2(n-k)} \tilde{\eta}^{2k} |n-k\rangle\langle n-k|. \end{aligned} \quad (22)$$

Written like this, we have described the POVM for the transmission of  $n$  photons, which yields possible detector outcomes ranging from 0 to  $n$ . However, we want the POVM corresponding to a *particular* photon-number detector reading  $k$ . We therefore have to reverse the rôles of  $n$  and  $k$  and adjust the summation in Eq. (22). The POVM for detecting  $k$  photons then becomes

$$\hat{E}_k = \sum_{n=k}^{\infty} \binom{n}{k} \eta^{2k} \tilde{\eta}^{2(n-k)} |n\rangle\langle n|. \quad (23)$$

The lowest three POVM's are given by

$$\hat{E}_0 = |0\rangle\langle 0| + \tilde{\eta}^2 |1\rangle\langle 1| + \tilde{\eta}^4 |2\rangle\langle 2| + \dots \quad (24a)$$

$$\hat{E}_1 = \eta^2 |1\rangle\langle 1| + 2\eta^2 \tilde{\eta}^2 |2\rangle\langle 2| + 3\eta^2 \tilde{\eta}^4 |3\rangle\langle 3| + \dots \quad (24b)$$

$$\hat{E}_2 = \eta^4 |2\rangle\langle 2| + 3\eta^4 \tilde{\eta}^2 |3\rangle\langle 3| + \dots \quad (24c)$$

Alternatively, instead of calculating the coefficients  $d_{k,l}$  of  $\hat{E}_k$  in a—necessarily simplified—model, these values can in principle be determined experimentally. This would take into account more subtle effects, such as the saturation properties of the detectors, and dark counts. Note that we can also include dark counts in our model by inserting a thermal state into the secondary input mode of the beam splitter. However, when we take detector readings only during small time windows, the dark count contribution becomes small, and the fidelity degradation is predominantly due to the detector inefficiencies.

To find the fidelity of the single-photon QND device, we have to combine Eq. (23) with Eqs. (17) and (18). For the output  $\rho_{\text{out}}$  in mode  $b'$  this yields

$$\rho_{\text{out}} = \text{Tr}_{a'c'd'} \left[ \hat{E}_0^{(a')} \otimes \hat{E}_1^{(c')} \otimes \hat{E}_1^{(d')} |\Psi\rangle\langle\Psi| \right], \quad (25)$$

that is, we condition the output on a detector coincidence in modes  $c'$  and  $d'$ , while nothing is detected in mode  $a'$ . When we evaluate this expression we find the (unnormalized) output density operator to be

$$\begin{aligned} \rho_{\text{out}} &= \frac{1}{8} \left( \eta^4 |c_1|^2 + \frac{3}{2} \eta^4 \tilde{\eta}^2 |c_2|^2 \right) |1\rangle\langle 1| \\ &\quad + \frac{1}{8} \left( \eta^4 \tilde{\eta}^2 |c_1|^2 + 3\eta^4 \tilde{\eta}^2 \right) |c_2|^2 |0\rangle\langle 0|. \end{aligned} \quad (26)$$

The normalization factor is given by

$$\frac{\eta^4}{8} \left[ (1 + \tilde{\eta}^2) |c_1|^2 + \left( \frac{5}{2} \tilde{\eta}^2 + 6\tilde{\eta}^4 \right) |c_2|^2 \right],$$

and the fidelity becomes

$$F = \frac{2 + 5\tilde{\eta}^2\gamma}{2 + \tilde{\eta}^2(2 + 5\gamma + 12\gamma\tilde{\eta}^2)}, \quad (27)$$

where  $\gamma \equiv |c_2|^2/|c_1|^2$  is the two-photon fraction in the input state with respect to the single-photon contribution. This fidelity depends on the input state, characterized by  $\gamma$ . For ideal detectors ( $\eta^2 = 1$ ) we find  $F = 1$ . In Fig. 4 we plotted the fidelity of the single-photon QND device as a function of the detector efficiencies for different values of  $\gamma$ . When we use the detectors from Ref. [23] with  $\eta^2 = 88\%$ , the fidelity is 89% for  $\gamma = 0$  and  $\gamma = 0.1$ , 86% for  $\gamma = 1$ , and 80% for  $\gamma = 10$ . The output state of the single-photon QND device is then

$$\rho_{\text{out}} = (1 - F)|0\rangle\langle 0| + F|1\rangle\langle 1|. \quad (28)$$

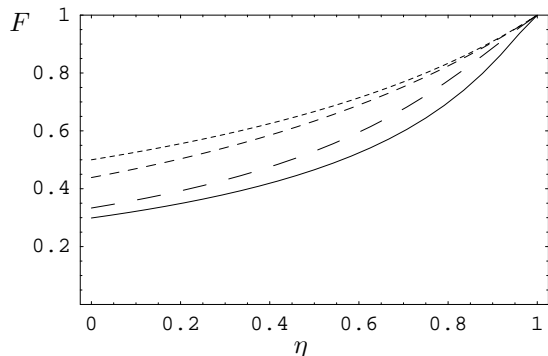


FIG. 4. The fidelity  $F$  as a function of the detector efficiency  $\eta$  for different values of  $\gamma$ . From the upper (dotted) curve to the lower (continuous) curve, the values of  $\gamma$  are 0, 0.1, 1, and 10 respectively.

It is immediately clear from Fig. 4 that this protocol works only when the detectors have a high quantum efficiency. In particular, when there is a sizeable two-photon contribution in the input state, the fidelity remains below 50% for most of the efficiency domain.

### C. Single-photon probes

We based the above fidelity calculation on perfect single-photon sources for the probe modes. When these modes are weak coherent states, the output fidelity deteriorates considerably. This is because we use *two* probes: For weak coherent states these two single-photon inputs occur with approximately the same probability as events with two probe photons in one mode and vacuum in the other. However, when we employ parametric down-conversion to create the two-photon states

that act as probes, this problem disappears. Given that the parametric down-converter creates the output state  $(1 - \epsilon^2)|0\rangle + \epsilon|1, 1\rangle + O(\epsilon^2)$ , the vacuum contribution of this state is eliminated in the post-selection process. Also, the efficiency of the whole QND device deteriorates rapidly (to order  $\sim 10^{-4}$ ), but this is still twelve orders of magnitude better than using bulk Kerr nonlinearities.

## III. POLARIZATION PRESERVING QND

So far, we have considered only optical fields in certain photon-number superpositions. You can argue that we can construct a single-photon “semi-QND” scheme by detecting the mode with a single-photon resolution detector and subsequently creating another photon with a single-photon gun. Indeed, this would work perfectly. However, when the incoming field has a certain unknown polarization that needs to be preserved, the semi-QND scheme breaks down. Our next goal is therefore to create an interferometric single-photon QND device that preserves the polarization of a photon  $|\theta\rangle \equiv \alpha|H\rangle + \beta|V\rangle$ , where  $\alpha$  and  $\beta$  are two complex numbers and  $H, V$  the polarization directions.

### A. Teleportation-based protocol

A simple and elegant way to create a polarization preserving QND device is to *teleport* the polarization state with the protocol used by Bouwmeester *et al.* [16]. As shown in Fig. 5, the incoming state  $|\psi_{\text{in}}\rangle = c_0|0\rangle + c_1|\theta\rangle$  (where  $|\theta\rangle = \alpha|H\rangle + \beta|V\rangle$ ) is mixed in a beam splitter with one half of a polarization entangled state from a parametric down-converter,  $|\Psi_{\text{PDC}}\rangle = (1 - \epsilon^2)|0\rangle + \epsilon(|H, V\rangle - |V, H\rangle)/\sqrt{2} + O(\epsilon^2)$ . Post-selection on a two-fold coincidence (the partial Bell detection) in detectors  $D_1$  and  $D_2$  yields the outgoing state  $|\theta\rangle$ .

The detector coincidence identifies the singlet state  $|\Psi^-\rangle \equiv (|H, V\rangle - |V, H\rangle)/\sqrt{2}$ . The complete set of Bell states is given by

$$\begin{aligned} |\Psi^\pm\rangle &= (|H, V\rangle \pm |V, H\rangle)/\sqrt{2}, \\ |\Phi^\pm\rangle &= (|H, H\rangle \pm |V, V\rangle)/\sqrt{2}. \end{aligned} \quad (29)$$

It is well known that a deterministic complete Bell state detection is impossible using linear optics [25], but we can construct a *probabilistic* Bell measurement that works with probability 1/2 using Ref. [26]. Unfortunately, the teleportation protocol breaks down when there is a (sizeable) two-photon contribution in the input state: When the incoming state is  $|\psi_{\text{in}}\rangle = c_0|0\rangle + c_1|\theta\rangle + c_2|2\theta\rangle$  (where  $|2\theta\rangle$  is the two-photon Fock state in the polarization mode  $\theta$ ), then the outgoing state  $\rho_{\text{tb}}$  based on a two-fold detector-coincidence (to first order in  $p_{\text{pdc}}$ ) is

$$\rho_{\text{tb}} = \frac{3p_{\text{pdc}}|c_1|^2}{4|c_2|^2 + 3p_{\text{pdc}}|c_1|^2} |\theta\rangle\langle\theta| + \frac{4|c_2|^2}{4|c_2|^2 + 3p_{\text{pdc}}|c_1|^2} |0\rangle\langle 0|, \quad (30)$$

where  $p_{\text{pdc}} \sim 10^{-4}$  is the probability of creating a single polarization-entangled photon pair in the parametric down-converter. The fidelity  $F = \text{Tr}[\rho_{\text{tb}}|\theta\rangle\langle\theta|]$  becomes vanishingly small when the two-photon contribution in the state increases (i.e., when  $|c_2|^2 \gg p_{\text{pdc}}|c_1|^2$ ). In the next section we shall study an interferometer that signals the presence of a single photon with arbitrary polarization even when there is a sizeable two-photon contribution present in the input state.

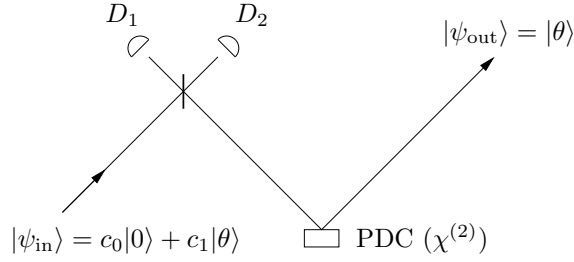


FIG. 5. Teleportation-based QND measurement device for single-photon detection that leaves the polarization of the photon intact. The device signals the presence of a single photon  $|\theta\rangle$  in the input mode with (three-dimensional) polarization angle  $\theta$ , by giving a detector coincidence in  $D_1$  and  $D_2$ .

## B. Two-photon robustness

We have just demonstrated that the teleportation-based protocol to perform polarization-invariant single-photon QND detections breaks down in the presence of a sizeable two-photon amplitude. Analogous to section II we now construct an interferometer that signals the presence of a single photon with arbitrary polarization when the input state is

$$|\psi_{\text{in}}(\theta)\rangle = c_0|0\rangle + c_1|\theta\rangle + c_2|2\theta\rangle, \quad (31)$$

where  $|\theta\rangle$  is a single photon with a polarization angle  $\theta$ . Note that  $\theta$  might be a two-dimensional vector so as to span the complete Bloch sphere. The term  $|2\theta\rangle$  denotes a two-photon state in the polarization mode corresponding to  $\theta$ .

Since the input mode can be in an arbitrary polarization state, we describe this as a two-mode input. The interferometer in Fig. 3 then works only if the single-photon auxiliary input states in modes  $c$  and  $d$  have the same polarization as mode  $a$ . As a consequence, this protocol cannot be used when the input polarization is unknown. Consider therefore the interferometric setup in Fig. 6.

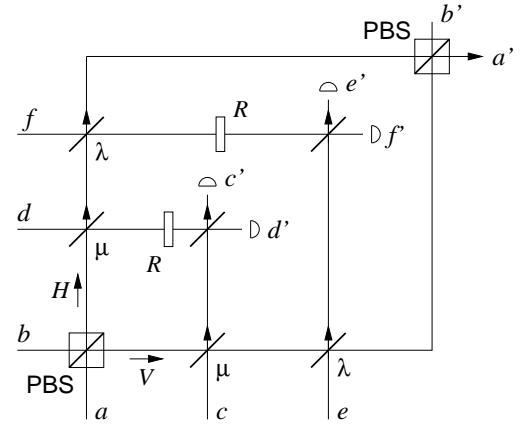


FIG. 6. The QND device for single-photon detection that leaves the polarization of the photon intact. Here, PBS denotes a polarization beam splitter and  $R$  is a polarization rotation over  $\pi/2$  to erase the which-path information in the detectors. A four-fold detector coincidence in modes  $c'$ ,  $d'$ ,  $e'$ , and  $f'$  (with one and only one photon per mode) signals the presence of a single photon in the input mode, while conserving the (unknown) polarization. The beam splitter coefficients are given by  $\mu = \lambda = \frac{1}{2} \arccos(-1/3)$ . The beam splitters before modes  $c'$ ,  $d'$ , and  $e'$ ,  $f'$  have transmission coefficients  $1/2$ .

Since the beam splitter can be represented by a simple  $SU(2)$  rotation around a fixed axis, we can parametrize the transmission coefficient  $T$  by the rotation angle  $\mu$  such that  $T = \cos^2 \mu$ . When we choose the angles  $\mu$  and  $\lambda$  for the different beam splitters according to

$$\mu = \lambda = \frac{1}{2} \arccos\left(-\frac{1}{3}\right) \quad \text{or} \quad T = \frac{1}{3}, \quad (32)$$

the mode transformations of this interferometer are

$$\hat{a}_H^\dagger \rightarrow \frac{1}{3} \left[ \hat{a}'_H^\dagger - \sqrt{3}(\hat{c}'^\dagger - \hat{d}'^\dagger) - \hat{e}'^\dagger + \hat{f}'^\dagger \right], \quad (33a)$$

$$\hat{a}_V^\dagger \rightarrow \frac{1}{3} \left[ \hat{a}'_V^\dagger - \sqrt{3}(\hat{c}'^\dagger + \hat{d}'^\dagger) - \hat{e}'^\dagger - \hat{f}'^\dagger \right], \quad (33b)$$

$$\hat{c}_V^\dagger \rightarrow \frac{2\hat{a}'_V^\dagger + \sqrt{3}(\hat{c}'^\dagger + \hat{d}'^\dagger) - 2(\hat{e}'^\dagger + \hat{f}'^\dagger)}{3\sqrt{2}}, \quad (33c)$$

$$\hat{d}_H^\dagger \rightarrow \frac{-2\hat{a}'_H^\dagger - \sqrt{3}(\hat{c}'^\dagger - \hat{d}'^\dagger) + 2(\hat{e}'^\dagger - \hat{f}'^\dagger)}{3\sqrt{2}}, \quad (33d)$$

$$\hat{e}_V^\dagger \rightarrow \frac{2\hat{a}'_V^\dagger + \hat{e}'^\dagger + \hat{f}'^\dagger}{\sqrt{6}}, \quad (33e)$$

$$\hat{f}_H^\dagger \rightarrow \frac{-2\hat{a}'_H^\dagger - \hat{e}'^\dagger + \hat{f}'^\dagger}{\sqrt{6}}. \quad (33f)$$

In this set of equations we dropped the index  $H, V$  of modes  $c'$ ,  $d'$ ,  $e'$ , and  $f'$ , since the polarizations of these modes are always identical.

Let the input state in mode  $a$  be given by Eq. (31), and feed probe photons with specified polarizations into

modes  $c$ ,  $d$ ,  $e$ , and  $f$ . The total input state  $|\Psi_{\text{in}}\rangle$  is then given by

$$\begin{aligned} |\Psi_{\text{in}}\rangle &= |\psi_{\text{in}}(\theta), 0, V, H, V, H\rangle_{abcdef} \\ &= \sum_{k=0}^2 c_k \hat{a}_\theta^{\dagger k} \hat{c}_V^\dagger \hat{d}_H^\dagger \hat{e}_V^\dagger \hat{f}_H^\dagger |0\rangle_{abcdef}. \end{aligned} \quad (34)$$

It is now a somewhat lengthy (but straightforward) calculation to show that when ideal detectors in modes  $c'$ ,  $d'$ ,  $e'$ , and  $f'$  all record a single photon, the input state collapses onto the single-photon state  $|\theta\rangle\langle\theta|$  in the output mode  $a'$ . Note that, due to the arrangement of the polarization beam splitters (PBS), the detection of mode  $b'$  is unnecessary: We do not have the problematic notion of conditioning on non-detection. The probability of a four-fold detector coincidence for a single-photon input in this polarization preserving single-photon QND device is  $(4/27)^2 \approx 2\%$ .

Suppose that the input field is in a polarization mode with  $|\theta\rangle = (|H\rangle + |V\rangle)/\sqrt{2}$ . Furthermore, define  $|\theta_\perp\rangle \equiv (|H\rangle - |V\rangle)/\sqrt{2}$ . When we use the realistic detectors modelled in Sec. II B we find the outgoing state to be approximately

$$\begin{aligned} \rho_{\text{out}} \propto & \left( \frac{\tilde{\eta}^2}{365} + \gamma \frac{\tilde{\eta}^4}{49} \right) |0\rangle\langle 0| \\ & + \left( \frac{16}{729} + \gamma \frac{\tilde{\eta}^2}{49} \right) |\theta\rangle\langle\theta| + \gamma \frac{\tilde{\eta}^2}{156} |\theta_\perp\rangle\langle\theta_\perp|, \end{aligned} \quad (35)$$

where  $\gamma \equiv |c_2|^2/|c_1|^2$ . For brevity, we have approximated the lengthy algebraic terms in this expression by fractions that are within 1% of their numerical value. Furthermore, the appearance of the term  $|\theta_\perp\rangle\langle\theta_\perp|$  does not indicate a polarization rotation associated with this interferometer; it merely indicates that imperfect detections tend to randomize the polarization of the output. After normalization the fidelity becomes approximately

$$F_\theta \approx \frac{1 + 0.93 \gamma \tilde{\eta}^2}{1 + (0.12 + 1.22 \gamma) \tilde{\eta}^2 + 0.93 \gamma \tilde{\eta}^4}. \quad (36)$$

We have plotted  $F_\theta$  as a function of the detector efficiency is shown in Fig. 7 for different values of  $\gamma$ . A property we immediately notice about this interferometer is that the fidelity is significantly more resilient to detector losses than the single-photon QND device for fixed polarization (see Fig. 4). When we calculate the fidelities of the output using the four different values of  $\gamma$ , we found that with  $\eta^2 = 88\%$ , the fidelity is 98.5% for  $\gamma = 0$ , 98% for  $\gamma = 0.1$ , 95% for  $\gamma = 1$ , and 81% for  $\gamma = 10$ .

We now have two criteria to select between teleportation based and interferometric QND detection: When we need a high-fidelity single-photon QND detection and the two-photon contribution is negligible, then we should use the teleportation-based quantum nondemolition device (Fig. 5). However, when we are in possession of

single-photon resolution detectors, or we need to exclude a sizeable two-photon contribution, the interferometric methods given in Figs. 3 and 6 are superior.

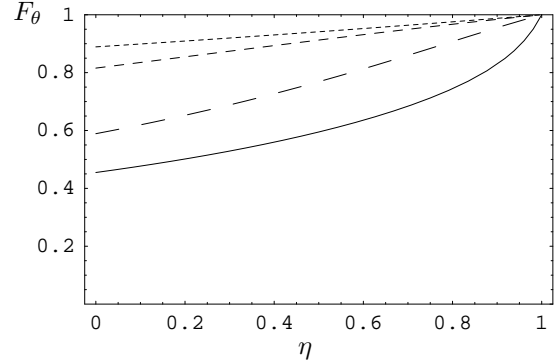


FIG. 7. The fidelity  $F_\theta$  as a function of the detector efficiency  $\eta$  for different values of  $\gamma$ . From the upper (dotted) curve to the lower (continuous) curve, the values of  $\gamma$  are 0, 0.1, 1, and 10 respectively.

#### IV. CONCLUSIONS

We have presented four, single-photon, quantum-nondemolition devices; two were based on polarization entanglement as an auxiliary input and two rely on single photons as auxiliary input states. A simple teleportation-based protocol allows us to perform a single-photon QND detection when the two-photon contribution in the input state is negligible. We presented an interferometer based on single-photon auxiliary input states and a two-fold detector coincidence that still works when the main input mode is populated by two photons. The optimal efficiency of this protocol is  $4/27$  or approximately 15%. In addition, we studied the effect of realistic detectors on the fidelity of the interferometer, and we found that existing detectors with 88% quantum efficiency and single-photon resolution may yield a fidelity of up to 89%, depending on the input state.

In the more general case where the polarization of the input mode matters, we can again use teleportation as our single-photon QND device. However, this protocol is still sensitive to two-photon pollution. We therefore constructed an interferometer that is both polarization preserving and that is robust against two-photon input states. This setup involves four-fold coincidence detection, and the efficiency is approximately 2%. However, this interferometer is not dependent on non-detection, contrary to the previous one, and as a consequence, the fidelity of the output state is considerably higher. For detectors with 88% efficiency we found output fidelities of up to 98%.

All of the above protocols are inherently frequency-independent. The question is now whether we can modify these schemes such that two-photon inputs and gen-

eral  $n$ -photon states can be identified without destroying them. This is the object of further study.

### ACKNOWLEDGEMENTS

This work was carried out at the Jet Propulsion Laboratory, California Institute of Technology, under a contract with the National Aeronautics and Space Administration. In addition, P.K. and H.L. acknowledge the United States National Research Council. Support was received from the Advanced Research and Development Activity, the National Security Agency, the Defense Advanced Research Projects Agency, and the Office of Naval Research.

---

\* pieter.kok@jpl.nasa.gov

- [1] J. von Neumann, *Mathematical Foundations of Quantum Mechanics*, Princeton University Press (1955).
- [2] P. Grangier, J.A. Levenson, and J.-P. Poizat, *Nature* **396**, 537 (1998). A. La Porta *et al.*, *Phys. Rev. Lett.* **62**, 28 (1989). J.-F. Roch *et al.*, *Phys. Rev. Lett.* **78**, 634 (1997). M. Brune *et al.*, *Phys. Rev. Lett.* **65**, 976 (1990); *Phys. Rev. A* **45**, 5193 (1992).
- [3] Q.A. Turchette, C.J. Hood, W. Lange, H. Mabuchi, and H.J. Kimble, *Phys. Rev. Lett.* **75**, 4710 (1995).
- [4] X. Maître, E. Hagley, G. Nogues, C. Wunderlich, P. Goy, M. Brune, J.M. Raimond and S. Haroche, *Phys. Rev. Lett.* **79**, 769 (1997).
- [5] N.J. Cerf, C. Adami, and P.G. Kwiat, *Phys. Rev. A* **57**, R1477 (1998).
- [6] E. Knill, R. Laflamme and G.J. Milburn, *Nature* **409**, 46 (2001).
- [7] B. Yurke *J. Opt. Soc. Am. B* **2**, 732 (1985).
- [8] G. Nogues, A. Rauschenbeutel, S. Osnaghi, M. Brune, J.M. Raimond and S. Haroche, *Nature* **400**, 239 (1999).
- [9] N. Imoto, H.A. Haus, and Y. Yamamoto *Phys. Rev. A* **32**, 2287 (1985).
- [10] See for example M.O. Scully and M.S. Zubairy, *Quantum Optics*, Cambridge University Press (1997).
- [11] B.C. Sanders and D.A. Rice, *Phys. Rev. A* **61**, 013805 (2000).
- [12] Z. Ou, *Phys. Rev. Lett.* **77**, 2352 (1996).
- [13] H. Lee, P. Kok, N.J. Cerf and J.P. Dowling, *Phys. Rev. A*, **65**, 030101(R) (2002); P. Kok, H. Lee and J.P. Dowling, *ibid.* 052104 (2002).
- [14] R.W. Boyd, *J. Mod. Opt.* **46**, 367 (1999).
- [15] M.D. Lukin and A. Imamoglu, *Phys. Rev. Lett.* **84**, 1419 (2000).
- [16] D. Bouwmeester, J.-W. Pan, K. Mattle, M. Eibl, H. Weinfurter and A. Zeilinger, *Nature* **390**, 575 (1997).
- [17] I.L. Chuang and Y. Yamamoto, *Phys. Rev. Lett.* **76**, 4281 (1996); A. Barenco *et al.*, *Phys. Rev. Lett.* **74**, 4083 (1995); A.P. Alodjants *et al.*, *Laser Phys.* **8**, 718 (1998).
- [18] J.C. Howell and J.A. Yeazell, *Phys. Rev. A* **62**, 032311 (2000).
- [19] G.J. Milburn and M.J. Gagen, *Phys. Rev. A* **46**, 1578 (1992).
- [20] P. Kok, C.P. Williams, and J.P. Dowling, [quant-ph/0203134](http://arxiv.org/abs/quant-ph/0203134).
- [21] S. Haroche, *Ann. NY Acad. Sci.* **755**, 73 (1995).
- [22] P. Kok and S.L. Braunstein, *Phys. Rev. A* **63**, 033812 (2001).
- [23] J. Kim, S. Takeuchi, Y. Yamamoto, and H.H. Hogue, *Appl. Phys. Lett.* **74** 902 (1999); *ibid.* 1063 (1999).
- [24] P. Kok and S.L. Braunstein, *Phys. Rev. A* **61**, 042304 (2000).
- [25] N. Lütkenhaus, J. Calsamiglia and K-A. Suominen, *Phys. Rev. A*. **59**, 3295 (1999); L. Vaidman and N. Yoran, *ibid.*, 116 (1999).
- [26] S.L. Braunstein and A. Mann, *Phys. Rev. A* **51**, R1727 (1995); *ibid.* **53**, 630 (1996).